



# Crystal and multiple melting behaviors of PCL lamellae in ultrathin films



Xiang Yu<sup>a</sup>, Na Wang<sup>a</sup>, Shanshan Lv<sup>b,\*</sup>

<sup>a</sup> College of Material and Chemical Engineering, Henan Institute of Engineering, Zhengzhou 450000, PR China

<sup>b</sup> College of Material Science and Engineering, Northeast Forestry University, Harbin 150040, PR China

## ARTICLE INFO

### Article history:

Received 21 August 2015

Received in revised form

14 December 2015

Accepted 21 December 2015

Communicated by R. Fornari

Available online 29 December 2015

### Keywords:

Poly ( $\epsilon$ -caprolactone) (PCL)

Atomic Force Microscope (AFM)

Ultrathin films

Multiple melting

## ABSTRACT

In this paper, isothermal crystallization at different temperatures and multiple melting of four molecular weights (*MW*) PCL ultrathin films were investigated by using Atomic Force Microscopy (AFM). The results showed that: two different crystal structures, Flat-on and Edge-on lamellae, were simultaneously formed in PCL ultrathin films when the  $T_c$  lower than 30 °C. During the heating process, Edge-on lamellae was melted firstly. This demonstrated that the multiple melting behavior of PCL in ultrathin films was caused by the two different lamellar structures. With the increase of *MW*, or with the decrease of  $T_c$ , PCL chains in ultrathin films changed from Flat-on to Edge-on, and the controlled factors of growth process in ultrathin films transformed from surface nucleation-limited (NL) to melt diffusion-limited (DL).

© 2015 Elsevier B.V. All rights reserved.

## 1. Introduction

Crystallization of polymers is one of the most intriguing topics in macromolecular physics [1]. In recent years, polymer crystallization in thin and ultrathin films has attracted increasing interest in both practical applications and scientific importance [2–5]. Polymer ultrathin films belong to the quasi-two-dimensional nanoscale materials, and the films thickness is less than 100 nm. Polymer restricted in ultrathin films, due to the interfacial effect and the space effect between films and substrate, and the crystallization behaviors are different from bulk crystallization, such as polymer chain orientation, crystal growth rate, crystallinity, crystal morphology [6,7], and so on.

During the crystallization process of polymer in ultrathin films, there are some affinities between the molecular chain and the substrate surface. Due to the influence of geometric constraints, when the phase transformation occurs, polymer chains tend to oriented growth in the vertical direction of the substrate surface, i.e. the lamellae's *c* axis (unit cell) is perpendicular to the substrate surface [8], this ordered crystal structure is termed Flat-on lamellae. In addition, the interaction force between the substrate surface and the polymer chains in ultrathin films is mostly from the interaction of polymer end group and substrate. It leads to the mobility of polymer chains dropping, the polymer chains arranged

in a preferred orientation during the crystallization process, are usually easier to growth Flat-on crystal. With the increase of the molecular weight, the proportion of polymer end group decreases, and the interaction between polymer chains and substrate also reduces, polymer chains incline to parallel to the substrate surface growth, now the growth of crystal is Edge-on, as shown in Fig. 1.

There are many influencing factors in the process of crystallization. It is generally thought that the growth kinetics of this system is usually controlled by two factors: nucleation-limited (NL) and diffusion-limited (DL). Each of these processes may be slower, with the variation of  $T_c$ , the processes compete with each other and ultimately affect the growth process and crystal morphology [9]. The two control processes depend largely on the  $T_c$ , when crystal at lower temperature, nucleation rate is quick and the segment movement ability is weak, so the nucleation rate is greater than the rate of diffusion, it is the melt diffusion controlled stage. With the increase of  $T_c$ , segment movement ability enhanced but the nucleation rate gradually decreased, the controlled factor of the crystal growth transition from DL to NL. When the  $T_c$  increases to a certain extent, melt diffusion become a faster process, the diffusion rate is larger than the nucleation rate, this moment is the surface nucleation controlled stage.

As we all know, a striking difference with respect to the behavior of a polymer and that of a low molecular compound concerns the melting process [10]. The compounds with low molecular weight have a well-defined melting temperature, while the polymer does not melt sharply at one particular temperature

\* Corresponding author.

E-mail address: [lvshpolymer@163.com](mailto:lvshpolymer@163.com) (S. Lv).

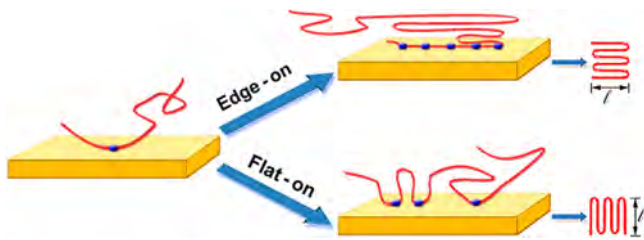


Fig. 1. The relationship between basement and molecular chain of polymer ultrathin film [8].

into clean liquid. Alternatively, it has a wide temperature range in the melting process. The appearance of multiple melting peaks is a long-standing phenomenon and still a controversial issue [11]. In particular, some semi-crystalline polymers often exhibit multiple melting behaviors during the heating process [12]. This interesting phenomenon, i.e. multiple melting transformation, has long been a hot spot in polymer physics, and in recent years, a large number of researches have appeared on the multiple melting transformation of various polymers, such as PA [11,13], PP [14], PET [15], PLLA [16–18], PEO [19] and so on. Chen et al. [19] used a low-molecular weight  $4250 \text{ gmol}^{-1}$  PEO fraction to analyze multiple melting by Atomic Force Microscopy (AFM) and Differential Scanning Calorimetry (DSC). The results showed that the melting and recrystallization behaviors occurred during heating process and led to multiple melting.

However, its mechanisms are not completely clear even now. The behavior may result from the following [20]: (a) the presence of more than one crystal structure model, (b) variation in morphology (such as lamellar thickness, distribution, perfection or stability), (c) melting–recrystallization–melting mechanism during DSC heating process, (d) physical aging or/and relaxation of the rigid amorphous fraction, (e) different molecular weight species, (f) orientation effects and so forth.

Poly ( $\epsilon$ -caprolactone) (PCL) is one of the most studied semi-crystalline thermoplastics due to its excellent biodegradability and biocompatibility. It has been widely used in many fields, such as tissue engineering materials [21,22], drug delivery and controlled release carrier [23], surgery [24] and so on, it even has potential applications in the field of biodegradable materials.

Although theoretical studies have illustrated the mechanism of crystal and multiple melting in bulk polymer, the limited set of experimental data in ultrathin films is still insufficient to understand the origin of the evolution of lamellae. Also, it is a novel method to characterize the multiple melting in the ultrathin films. In this paper, we describe and analysis the crystal evolution and multiple melting in ultrathin films of PCL with four kinds of molecular weight (MW) by using AFM. The effect of isothermally crystallized temperature ( $T_c$ ) and MW on the phenomenon of multiple melting were systematically discussed.

## 2. Experimental

### 2.1. Materials and sample preparation

PCL materials were supplied by JiNan Biochemical Co. Ltd. (China). Before the experiments, PCLs were carried out three times precipitation fractionations in order to get narrower the molecular weight distribution (MWD) of PCL (Solvent: Tetramethylene oxide (THF), Precipitating agent: petroleum benzin).

### 2.2. Characterization

#### 2.2.1. Molecular weight characterize

The  $M_n$  and MWD ( $M_w/M_n$ ) of fractionated samples were determined by GPC (Waters 2410) with Waters styragel column (The aperture is  $10^3 \text{ \AA}$ ,  $10^4 \text{ \AA}$  and  $10^5 \text{ \AA}$ , respectively). The  $M_n$  of samples is about  $0.5 \times 10^4$ ,  $0.8 \times 10^4$ ,  $2.5 \times 10^4$  and  $5.1 \times 10^4$ , respectively. And all of the samples' MWD are less than 1.5.

#### 2.2.2. Differential Scanning Calorimetry (DSC)

A TA Q2000 Differential Scanning Calorimetry (DSC) apparatus was used for the thermal analysis of Samples. The calibration of temperature scale and heat flow was carried out the melting scans of high-purity indium and zinc standard materials at the same heating rate ( $5 \text{ }^\circ\text{C/min}$ ). In the experiment, about 3~5 mg of the sample was weighed and sealed in an aluminum pan. By using DSC, the sealed sample was heated to  $80 \text{ }^\circ\text{C}$  for eliminating the heat history completely, and it was quenched to  $T_c$ s (the isothermal crystallization temperature) for the complete crystallization. Finally, the heating curves were scanned by DSC at the heating rate of  $5 \text{ }^\circ\text{C/min}$ .

#### 2.2.3. Atomic Force Microscopy (AFM)

The model of AFM which was used in this experiment is BenYuan CSPM-5500, China Guangzhou BenYuan nanometer Instrument Company. The instrument is equipped with a hot stage, sample can be tested in situ heating and cooling, the accuracy is  $0.1 \text{ }^\circ\text{C}$ . Moreover, the instrument includes software Imager 4.7 which can process data online and offline. In the experiments, Nano Devices RTESP tapping-mode silicon probe was used, all experiments were tested at the scanning range of  $15 \mu\text{m} \times 15 \mu\text{m}$  and  $512 \times 512 \text{ pixel}^2$ , the scanning rate is 2 Hz.

Before the AFM testing,  $0.25 \text{ mg mL}^{-1}$  PCL solution was prepared, then dropped 1–2 drops of the solution on the mica surface, simultaneously dried 12 h under vacuum. Placed the prepared sample on the heating stage for 3–5 min at  $80 \text{ }^\circ\text{C}$  to eliminate the thermal history thoroughly, then quenched to the setting temperature and isothermally crystallized for 30 min, finally investigated by AFM.

## 3. Results and discussion

### 3.1. The temperature dependence of PCL multiple melting

Fig. 2 was DSC heating curves of PCL- $2.5 \times 10^4$  isothermally crystallized at  $T_c$ s ( $-30 \text{ }^\circ\text{C}$  to  $40 \text{ }^\circ\text{C}$ ). As shown in it, when the  $T_c$  was lower than  $30 \text{ }^\circ\text{C}$ , all the curves had two melting peaks, in other words, multiple melting transformation took place. With the increasing of  $T_c$ , the lower  $T_m$  increased, and the higher  $T_m$  changed a little (shown in Fig. 3(a)). The peak height ratio of the lower to the higher decreased as the  $T_c$  increasing, as shown in Fig. 3(b). When the  $T_c$  was at or above  $30 \text{ }^\circ\text{C}$ , the higher melting peak disappeared. In addition, the melting range decreased when the  $T_c$  increased. The results indicated that more perfect and uniform crystal could be got with the rise of temperature. Therefore, we might divide the PCL melting behaviors into two types, mono-melting and dual-melting, according to  $T_c$ .

### 3.2. Phase transition of PCL in ultrathin films during heating process

Based on the above DSC experimental results, we systematically investigated the heating process of PCL- $2.5 \times 10^4$  ultrathin films isothermally crystallized at  $T_c$  lower than  $30 \text{ }^\circ\text{C}$ . Here, we only analyzed the heating process of ultrathin films prepared at

20 °C. The sample morphology was in situ and real time scanning by AFM at a heating rate of 5 °C/min.

The AFM height images of PCL ultrathin films which were isothermally crystallized at 20 °C were shown in Fig. 4(a). As can be seen in Fig. 4(a), two different morphological lamellae, Flat-on (flake-like) and Edge-on (fiber-like), can be observed at the same time. Moreover, most of the Edge-on and Flat-on connected to each other. As shown in Fig. 4(b) (c) and (d), the Edge-on crystal gradually disappeared when the temperature increased. When the temperature reached 55 °C, the Edge-on crystal was completely melted, but the Flat-on did not show obvious collapsibility. When the temperature was increased to 57 °C, all the lamellae transformed into melting state and flocked together, and its periphery was smooth, as shown in Fig. 4(d). The similar report has been published [19], with the increase of the temperature, the edges of lamellae became smooth and the Flat-on lamellae was thickened which led to a later melting of the lamellae. In addition, the recrystallization probably occurred during the heating process, which also could exhibit multiple melting phenomenon.

In conclusion, there were two lamellar structures in the ultrathin films prepared at low temperature, and the lamellae had different  $T_m$ . Comparing the surface free energy of these two lamellae, the surface free energy of Edge-on crystal was obviously larger than that of the Flat-on crystal [1,25,26], as shown in the Eqs. (2) and (3).

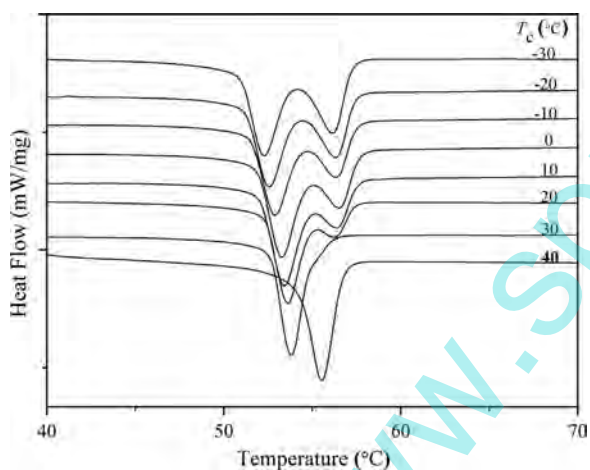


Fig. 2. DSC heating curves of PCL- $2.5 \times 10^4$  isothermally crystallized at  $T_c$ s (–30 °C to 40 °C).

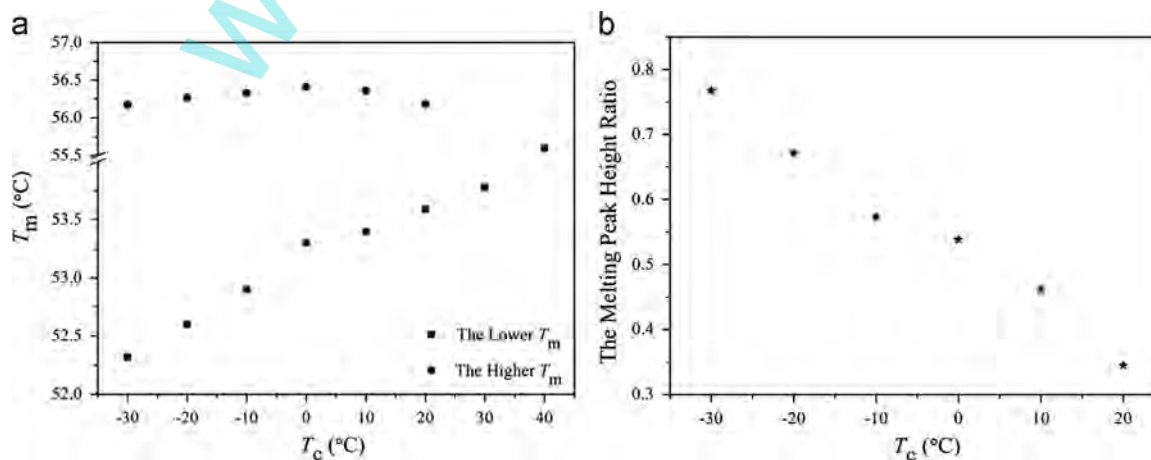


Fig. 3. (a) The relationship between  $T_c$  and (a)  $T_m$ ; (b) the melting peak height ratio of the lower to the higher of PCL- $2.5 \times 10^4$ .

Edge-on:

$$\sigma_e(\text{Edge on}) = G_{\text{upper}} + G_{\text{lower}} + G_{\text{lateral}} \quad (1)$$

In this equation,  $G_{\text{upper}}$  is upper surface free energy;  $G_{\text{lower}}$  is lower surface free energy;  $G_{\text{lateral}}$  is lateral surface free energy.

Due to  $G_{\text{upper}} = G_{\text{lower}} > G_{\text{lateral}}$

Consequently

$$\sigma_e(\text{Edge on}) = 2G_{\text{upper}} \quad (2)$$

The same to Flat-on:

$$\sigma_e(\text{Flat on}) = G_{\text{upper}} \quad (3)$$

This is because the Flat-on crystal is perpendicular to the substrate surface, it only has one surface; but the Edge-on crystal is parallel to the substrate surface, so it has two surfaces.

The effect of surface free energy on  $T_m$  is obvious, according to equation of Gibbs–Thomson [26]:

$$T_m = T_m^0(\infty)[1 - 2\sigma_e/(l\Delta h_f)] \quad (4)$$

The larger the lamellar thickness, the higher the  $T_m$  was, but the surface free energy was lower. Therefore, with the decrease of surface energy, the  $T_m$  progressively increased.

In summary, during the process of crystalline phase transition in the quasi two-dimensional space, there were multiple paths for the molecular chains to discharge into the crystal lattices, thus formed a variety of crystals, and these crystals had different physical properties. First of all, the molecular chains tended to grow relatively stable lamellae, i.e. Flat-on crystal. But at lower temperature, when the molecular chains discharged into the crystal lattice, the direction of chains could change easily because of the decline of molecular thermal movement. And it led to grow two kinds of lamellae with different surface free energy, i.e. these lamellae had different  $T_m$ . Obviously this is the internal reason which led to the multiple melting of PCL ultrathin films crystal. It supported that: when the lamellae was prepared at low temperature, it were easy for the molecular chains to grow imperfect crystal (the surface free energy is high) due to the greater driving force of crystallization and the weaker movement ability of segment. Ultimately, the imperfect crystal was melted first during the heating process, as the temperature increased, other perfect crystal was melted. Above all, this part of the experiment could support the multiple melting transformation mechanism from another perspective.

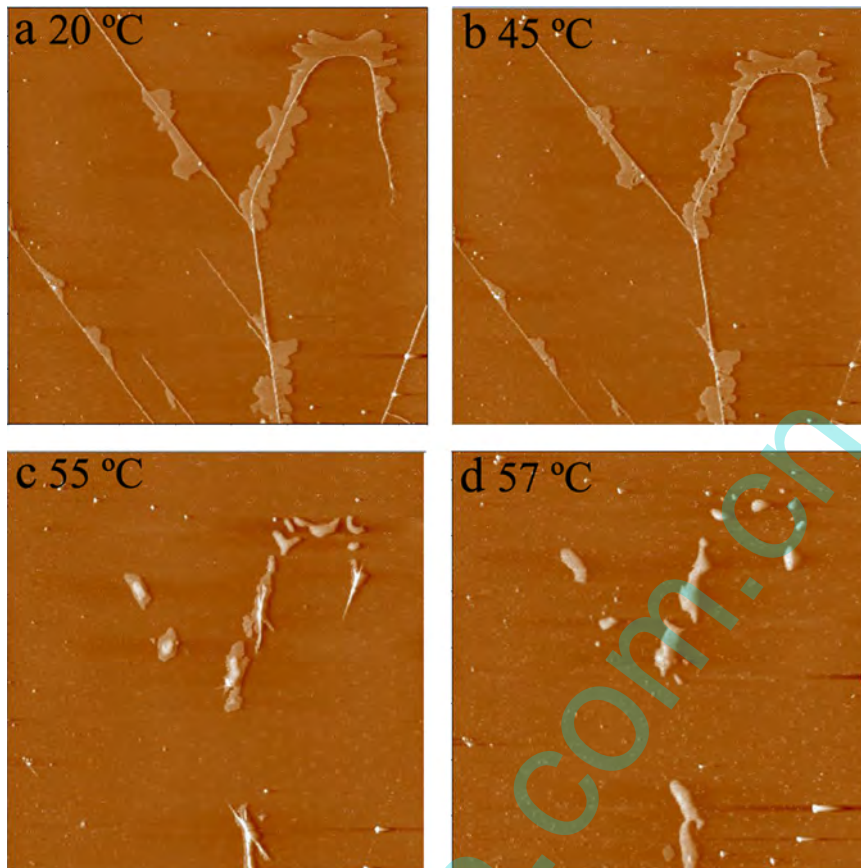


Fig. 4. AFM height images of PCL isothermally crystallized at 20 °C during heating process (15  $\mu\text{m} \times 15 \mu\text{m}$ ).

### 3.3. The effect of $T_c$ on PCL ultrathin films morphologies

As we all know, the crystallization temperature can affect the orientation of the lamellae formed in ultrathin film on solid substrates [27]. Fig. 5 is the AFM height images of PCL ultrathin films isothermally crystallized from  $-20 \text{ }^\circ\text{C}$  to  $30 \text{ }^\circ\text{C}$ , the scanning range was  $15 \mu\text{m} \times 15 \mu\text{m}$ . As can be seen in Fig. 5, when  $T_c$  was low, a large number of Edge-on crystal existed, and along with the increase of  $T_c$ , the number of Flat-on crystal increased while the number of Edge-on crystal reduced, accompanying with the transformation of crystal surface from rough to smooth.

As we all know, the crystallization process requires a certain degree of crystallization driving force (undercooling,  $\Delta T$ ) to overcome the potential barrier of nucleation [28,29], and  $\Delta T = T_m - T_c$ , so  $T_c$  is an important factor to affect the crystal morphologies. With the increase of  $T_c$ , crystal growth was affected by two aspects, namely, the nucleation rate gradually decreased and the diffusion rate increased. During the nucleation process, Edge-on nucleus and Flat-on nucleus were both induced to grow, and Edge-on nucleus' dependence on supercooling was more obvious, i.e. with the increase of  $T_c$ , Edge-on crystal nucleus number decreased gradually, the number of the Edge-on crystal also reduced progressively. During the process of crystal growth, when the temperature rose, the molecular diffusion speed was accelerated, and spread to the Flat-on crystal nucleus whose thermo-dynamic properties were more stable. As shown in the images, with the increase of  $T_c$ , the number of Flat-on crystal had a gradual increase.

On the other hand, with the increase of  $T_c$ , the facet of Flat-on crystals turned from rough to smooth. The reason of this was the growth process of crystal had two main controlling factors:

nucleation control (NL) and diffusion control (DL) [30]. The two processes might both be slow, with the variances of  $T_c$ , these processes competed with each other and finally the dominant process decided the growth process of crystal. When the crystallization temperature was very low, the fiber-like crystals (Edge-on) were formed, as shown in Fig. 5(a). When the  $T_c$  was  $0 \text{ }^\circ\text{C}$  (Fig. 5(c)), the number of fiber-like crystals decreased significantly. Especially, there was only one morphology lamellae (Flat-on) at  $30 \text{ }^\circ\text{C}$  (Fig. 5(f)), so it had merely one  $T_m$ , which agreed with the result of DSC (see Section 3.1). This showed that: when  $T_c$  was lower, the crystal nucleation rate was fast, while the chain segment movement ability was so weak that the melt diffusion rate was too slow. Thus, this process controlled by the melt diffusion resulted in the asperities of lamellae's lateral surface. With the increase of  $T_c$ , the nucleation rate gradually decreased and the melt diffusion rate improved little by little. When the  $T_c$  was higher, the growth process of lamellae was completely controlled by nucleation, and the lamellae's periphery became smooth. The similar result has been reported by Zhang et al. [31].

Through the above analysis,  $T_c$  was a crucial factor in the PCL ultrathin films morphologies. Specifically, Flat-on and Edge-on lamellae grow simultaneously at lower  $T_c$  while only Flat-on at higher  $T_c$ . With the decrease of  $T_c$ , the segment movement ability was weaker, when the molecular chains discharged into the crystal lattice, the direction of chains could change easily, resulting in the gradually increased number of Edge-on crystal. Because of the difference in  $T_m$  between Edge-on and Flat-on, the multiple melting transition phenomenon became more and more obvious with the rise of  $T_c$ .

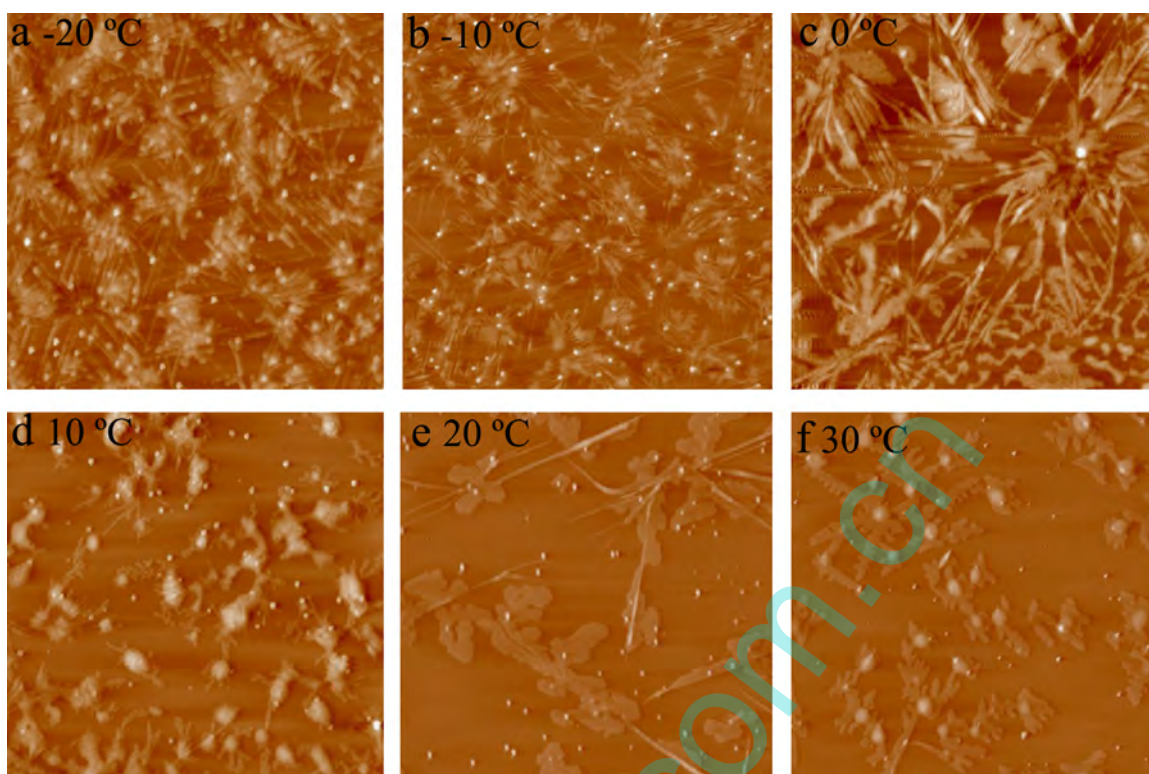


Fig. 5. AFM height images of PCL isothermally crystallized at different  $T_c$  ( $15 \mu\text{m} \times 15 \mu\text{m}$ ).

#### 3.4. The effect of molecular weight (the same $T_c$ ) on PCL ultrathin film morphologies

PCL ultrathin films with four different molecular weights prepared at  $0^\circ\text{C}$  were studied as an example, the surface morphology was observed by AFM (scanning range is  $15 \mu\text{m} \times 15 \mu\text{m}$ ), as shown in Fig. 6. As can be seen in Fig. 6(a), (b) and (c), there were two kinds of structures (some flake-like crystal (Flat-on) and some straight fiber-like crystal (Edge-on)) existed in the morphologies. In addition, the shape of Flat-on was irregular and the color was similar. Moreover, most of Flat-on lamellae and Edge-on lamellae connected and influenced with each other, reflecting that the direction of molecular chains changed when the lamellae formed.

With the increase of MW, the number of Edge-on gradually increased. This can be attributed to the orientation mechanism and segment movement ability in the ultrathin films. The orientation direction of lamellae was related to the interaction force between the interface of ultrathin films and the molecular chains. When the force was strong, it was favorable for the growth of Flat-on crystal. It can be explained as follows: the molecular chains movement ability was weak on the interface, only leading to the formation of Flat-on lamellae, on which inhibited effect was weak, rather than that of Edge-on crystal nucleus. The most induced effect of interface came from end-group. When the molecular weight was smaller, the proportion of end-group was larger, and the interfacial effect was more obvious. Therefore, Flat-on nucleus could form alone and induced smooth lamellae. As the molecular weight increased, the proportion of end-group declined gradually, the interfacial effect also decreased, it could form both Edge-on nucleus and Flat-on nucleus, and with the increase of molecular weight, Edge-on crystal nucleus increased gradually, leading to the increase of Edge-on crystal. When the molecular weight increased to 51,000, most of the crystal was Edge-on, showing that most molecular chains of PCL lamellae were growing parallel to the mica substrate surface, as shown in Fig. 6(d). At the same time, due

to the high molecular weight, the chains were so strongly intertwined and entangled that the segment mobility decreased, molecular chains could not discharge into the lattice regularly. During the phase transition process, the direction of molecular chains changed easily. Thus, both sides of the Edge-on could induce to grow Flat-on lamellae, and when the Flat-on grew to a certain extent, the direction of molecular chains changed on its boundary again, resulting in growing Edge-on lamellae.

In addition, as shown in the Fig. 6(d), many adjacent bunch of Edge-on lamellae could grow parallel to each other. This was because the lamellae had shearing functions to the adjacent melt, namely the melt surrounding the lamellae was pre-orientation state, so both sides of the lamellar were more likely to induce a new nucleation and crystal growth. Generally speaking, when isothermally crystallized at low temperature, the crystals were irregular. The possible reason was that the nucleation speed was fast at low temperature, resulting in forming numerous nuclei, including the Edge-on nuclei and the Flat-on nuclei, and molecular chains motion ability was low, it was unable to form perfect lamellae. To sum up, with the increase of molecular weight, the number of Edge-on crystal was also on the rise, more unstable crystal existed in the system, the multiple melting transition phenomenon was more easily to take place.

#### 3.5. The relationship between the thickness and $T_c$

Lamellar thickness was one of the most direct parameters that reflect the polymer crystal properties, especially thermal stability. Moreover, different thickness and thickness distribution of the lamellae were formed at different  $T_c$ . In this part, the multiple melting transformation was illustrated by the thickness and thickness distribution of Flat-on crystal in other way. In general, when the distribution of thickness was wider, the melting range was wider and the multiple melting transition was more obvious.

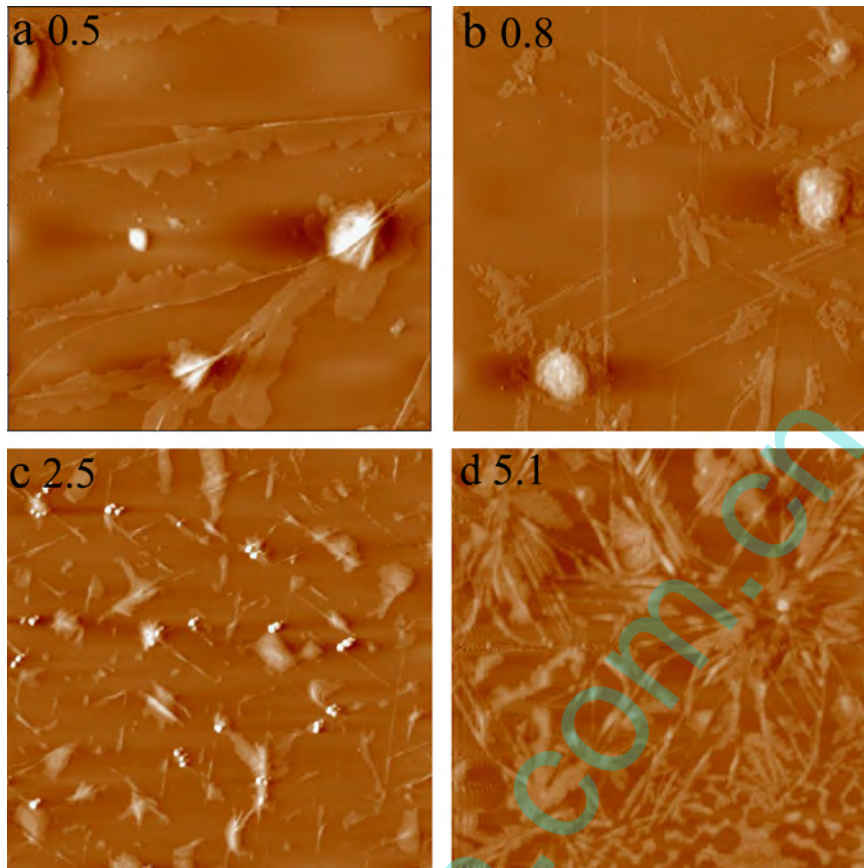


**Fig. 6.** AFM height images of PCL with different molecular weight ( $10^4$ ) isothermally crystallized at 0 °C ( $15 \mu\text{m} \times 15 \mu\text{m}$ ).

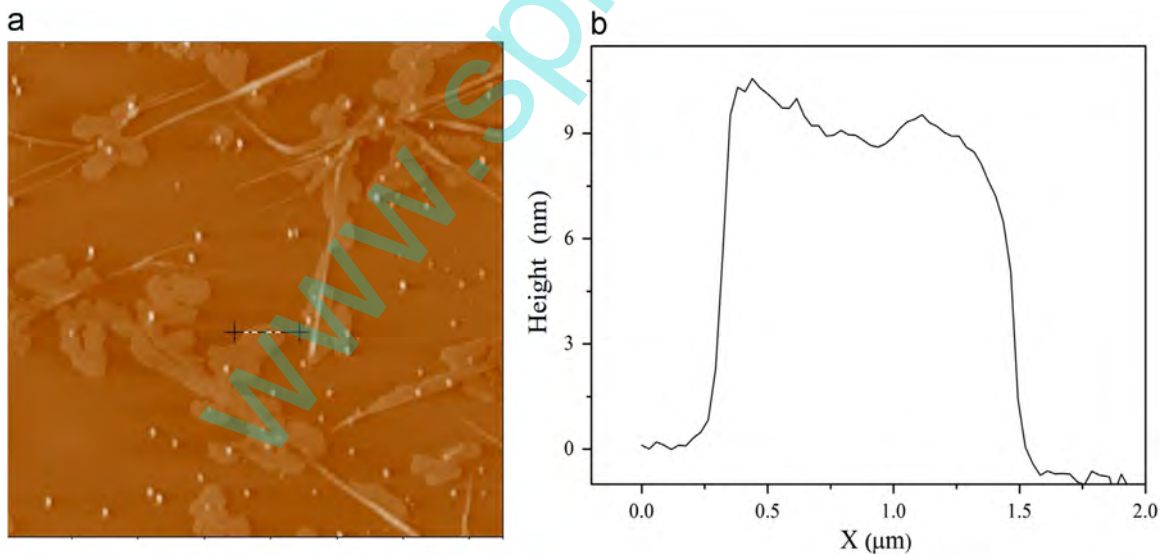


**Fig. 7.** (a) AFM height image of PCL- $2.5 \times 10^4$  isothermally crystallized at 20 °C ( $15 \mu\text{m} \times 15 \mu\text{m}$ ); (b) The relationship between height and AFM scanning hatched line of Fig. 7 (a).

Fig. 7 was the AFM height images of PCL- $2.5 \times 10^4$  ultrathin films isothermally crystallized at 20 °C and the lamellar thickness measured by AFM software. Fig. 7(b) was the relationship between the absolute height and scanning range of the position which was marked by vernier in Fig. 7(a). The lamellar thickness was 9.29 nm which was calculated based on the height average of Flat-on lamellae according to Fig. 7(b).

The distribution pattern showed in Fig. 8(a) was the nonlinear fitting of height distribution histogram which was gotten by the statistic of all lamellar thickness in Fig. 7(b). The lamellar thickness distribution could be reflected by  $K$  which was the ratio of peak height and half peak width in Fig. 8(a), and  $K = 18.75$ . Fig. 8 (b) was obtained by the same data processing of samples prepared at other  $T_c$ .

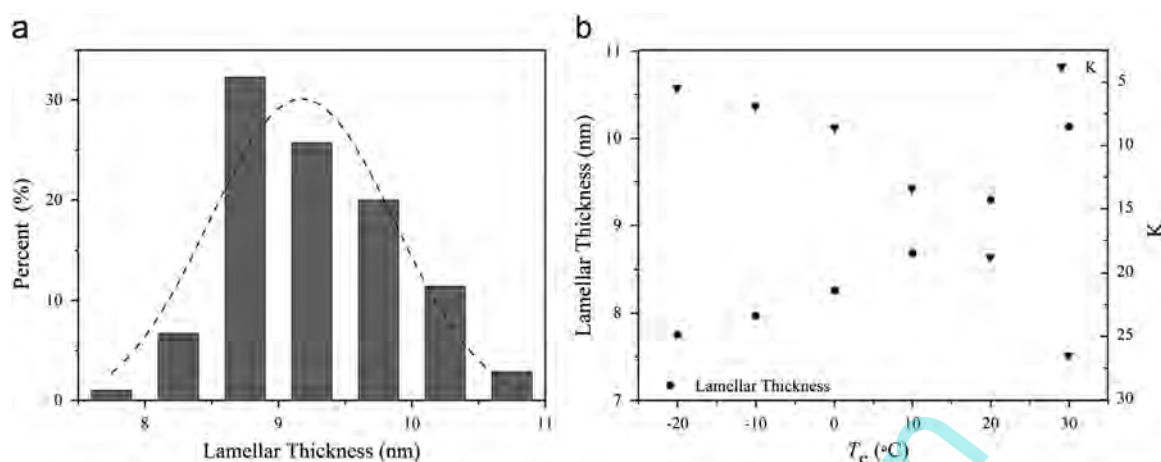


Fig. 8. (a) The lamellae thickness distribution; (b) The lamellar thickness and  $K$  as a function of  $T_c$  ( $K$  is the ratio of peak height and half peak width in Fig. 8(a)).

As shown in Fig. 8(b), the lamellar thickness and  $K$  all increased with  $T_c$ . On the one hand, it reflected the relationship between  $T_c$  and lamellar thickness. And the lamellar thickness increased from 7.75 nm to 10.13 nm. On the other hand, it demonstrated the regularity of lamellar thickness according to  $K$  value. The lamellar thickness had a decisive influence on its  $T_m$ . When the crystal was prepared at low temperature, the undercooling was high, so it was easy to form a variety of crystal nucleus with different sizes which would lead to forming different structures and thicknesses of lamellae. What's more, the chains movement ability was so weaker at lower  $T_c$  that a variety of lamellae with different structures and regularity formed when the molecular chains discharge into the crystalline region. All of those may lead to the multiple melting transformation.

#### 4. Conclusions

The melting process of PCLs prepared at lower  $T_c$  was in-situ researched by AFM. And the dependence of the multiple melting of PCL on  $T_c$  and  $MW$  was systematically investigated by using DSC and AFM. In ultrathin films, there were two different morphologies, Flat-on lamellae and Edge-on lamellae, when PCLs were prepared at  $T_c$  lower than 30 °C. And during the melting process, the Edge-on lamellae melt first, and then the Flat-on lamellae disappear gradually. It showed that the multiple melting behavior in PCL ultrathin films took place due to the two different structures, Flat-on lamellae and Edge-on lamellae. With the decrease of  $T_c$ , or with the increase of  $MW$ , the amount of Edge-on lamellae increased, and the multiple melting behavior became more obvious. Furthermore, the multiple melting phenomenon was illustrated according to the regularity of lamellae thickness from another point view. With the rise of  $T_c$ , the regularity of lamellar thickness increased. In conclusion, with the decrease of  $T_c$ , or with the increase of  $MW$ , nucleation process should be fast, and molecular movement should be limited to diffuse slowly. In this condition, there were many different paths of phase transition to form a variety of lamellae with different morphologies and different thickness, which were significant influencing factors on polymer multiple melting transformation.

#### Acknowledgments

The authors acknowledge the Joint Funds of the National Natural Science Foundation of China-Henan province people's

Government (No. U1304213) and the Doctor Fund of Henan Institute of Engineering (No. 2012029) for their financial support.

#### References

- [1] S.Z.D. Cheng, *Phase Transitions in Polymers: The Role of Metastable States*, Elsevier, Amsterdam, 2008.
- [2] Z.P. Ma, G.L. Zhang, X.M. Zhai, L.X. Jin, X.F. Tang, P. Zheng, W. Wang, Fractal crystal growth of poly (ethylene oxide) crystals from its amorphous monolayers, *Polymer* 49 (2008) 1629–1634.
- [3] Y.X. Liu, J.F. Li, D.S. Zhu, E.Q. Chen, H.D. Zhang, Direct observation and modeling of transient nucleation in isothermal thickening of polymer lamellar crystal monolayers, *Macromolecules* 42 (2009) 2886–2890.
- [4] G.L. Zhang, L.X. Jin, P. Zheng, A.C. Shi, W. Wang, Labyrinthine pattern of polymer crystals from supercooled ultrathin films, *Polymer* 51 (2010) 554–562.
- [5] L.X. Jin, G.L. Zhang, X.M. Zhai, Z.P. Ma, P. Zheng, W. Wang, Macromolecular effect on crystal pattern formation in ultra-thin films: molecular segregation in a binary blend of PEO fractions, *Polymer* 50 (2009) 6157–6165.
- [6] K.S. Tiaw, S.H. Teoh, R. Chen, M.H. Hong, Processing methods of ultrathin poly ( $\epsilon$ -caprolactone) films for tissue engineering applications, *Biomacromolecules* 8 (2007) 807–816.
- [7] H. Schönherr, C.W. Frank, Ultrathin films of poly (ethylene oxides) on oxidized silicon. 1. Spectroscopic characterization of film structure and crystallization kinetics, *Macromolecules* 36 (2003) 1188–1198.
- [8] A. Hershkovits-Mezuman, H. Harel, Y.T. Wang, C.H. Li, J.C. Sokolov, M.H. Rafailovich, G. Marom, The effects of interfacial interactions on lamellar morphologies in thin and ultrathin films and nanocomposites of LLDPE, *Compos. A – Appl. Sci. Manuf.* 41 (2010) 1066–1071.
- [9] J.J. Point, A new theoretical approach to the secondary nucleation at high supercooling, *Macromolecules* 12 (1979) 770–775.
- [10] V.R. Gowariker, N.V. Viswanathan, J. Sreedhar, *Polymer Science*, Wiley&Sons, New York, 1986.
- [11] J.B. Song, Q.Y. Chen, M.Q. Ren, X.H. Sun, H.L. Zhang, H.F. Zhang, S.Y. Wang, Z.S. Mo, Multiple melting and crystallization behavior of Nylon 1212, *Chin. J. Polym. Sci.* 24 (2006) 187–193.
- [12] M. Yasuniwa, S. Tsubakihara, T. Fujioka, Y. Dan, X-ray studies of multiple melting behavior of poly (butylene-2,6-naphthalate), *Polymer* 46 (2005) 8306–8312.
- [13] G.F. Shan, W. Yang, X.G. Tang, M.B. Yang, B.H. Xie, Q. Fu, Y.W. Mai, Multiple melting behaviour of annealed crystalline polymers, *Polym. Test.* 29 (2010) 273–280.
- [14] X.X. Li, H.Y. Wu, J.W. Chen, J.H. Yang, T. Huang, N. Zhang, Y. Wang, Non-isothermal crystallization and multiple melting behaviors of ss-nucleated impact-resistant polypropylene copolymer, *J. Appl. Polym. Sci.* 126 (2012) 1031–1043.
- [15] B. Mallick, R.C. Behera, S. Panigrahi, T.N. Tiwari, Effect of proton irradiation on multiple melting peaks of polyethylene terephthalate, *J. Mater. Sci.* 42 (2007) 2198–2199.
- [16] Y. Munehisa, S. Kazunari, O. Yoshinori, K. Wataru, Melting behavior of poly (l-lactic acid): X-ray and DSC analyses of the melting process, *Polymer* 49 (2008) 1943–1951.
- [17] C.Y. Shen, Y.M. Wang, M. Li, D.F. Hu, Crystal modifications and multiple melting behavior of poly (L-lactic acid-co-D-lactic acid), *J. Polym. Sci. Polym. Phys.* 49 (2011) 409–413.
- [18] Z.Y. Wei, P. Song, C. Zhou, G.Y. Chen, Y. Chang, J.F. Li, W.X. Zhang, J.C. Liang, Insight into the annealing peak and microstructural changes of poly (L-lactic acid) by annealing at elevated temperatures, *Polymer* 54 (2013) 3377–3384.

- [19] E.Q. Chen, A.J. Jing, X. Weng, P. Huang, S.W. Lee, S.Z.D. Cheng, B.S. Hsiao, F. Yeh, In situ observation of low molecular weight poly (ethylene oxide) crystal melting recrystallization, *Polymer* 44 (2003) 6051–6058.
- [20] T. Liu, J. Petermann, Multiple melting behavior in isothermally cold-crystallized isotactic polystyrene, *Polymer* 42 (2001) 6453–6461.
- [21] J.P. Lin, J.Q. Zhu, T. Chen, S.L. Lin, C.H. Cai, L.S. Zhang, Y. Zhuang, X.S. Wang, Drug releasing behavior of hybrid micelles containing polypeptide triblock copolymer, *Biomaterials* 30 (2009) 108–117.
- [22] X.X. Han, J.Z. Pan, A model for simultaneous crystallization and biodegradation of biodegradable polymers, *Biomaterials* 30 (2009) 423–430.
- [23] E. Chiellini, A. Corti, A. Giovannini, P. Narducci, A.M. Paparella, R. Solaro, Evaluation of biodegradability of poly ( $\epsilon$ -caprolactone)/poly (ethylene terephthalate) blends, *J. Env. Polym. Degrad.* 4 (1996) 37–50.
- [24] C.I. Winternitz, J.K. Jackson, A.M. Oktaba, H.M. Burt, Development of a polymeric surgical paste formulation for taxol, *Pharm. Res.* 13 (1996) 368–375.
- [25] Y. Wang, M. Rafailovich, J. Sokolov, D. Gersappe, T. Araki, Y. Zou, A.D.L. Kilcoyne, H. Ade, G. Marom, A. Lustiger, Substrate effect on the melting temperature of thin polyethylene films, *Phys. Rev. Lett.* 96 (2006) 28303–28306.
- [26] H. Marand, J.D. Hoffman, Determination of the fold surface free energy and the equilibrium melting temperature for  $\alpha$ -phase poly (pivalolactone) crystals, *Macromolecules* 23 (1990) 3682–3687.
- [27] L.W. Zhong, X.K. Ren, S. Yang, E.Q. Chen, C.X. Sun, A. Stroeks, T.Y. Yang, Lamellar orientation of polyamide 6 thin film crystallization on solid substrates, *Polymer* 55 (2014) 4332–4340.
- [28] S. Couch, R.S.J. Sparks, M.R. Carroll, The kinetics of degassing-induced crystallization at Soufriere Hills Volcano, Montserrat, *J. Petrol.* 44 (2003) 1477–1502.
- [29] E. Mollard, C. Martel, J.L. Bourdier, Decompression-induced crystallization in hydrated silica-rich melts: empirical models of experimental plagioclase nucleation and growth kinetics, *J. Petrol.* 53 (2012) 1743–1766.
- [30] Y.X. Liu, E.Q. Chen, Polymer crystallization of ultrathin films on solid substrates, *Coord. Chem. Rev.* 254 (2010) 1011–1037.
- [31] G. Zhang, Y. Cao, L. Jin, P. Zheng, R.M. Van Horn, B. Lotz, S.Z.D. Cheng, W. Wang, Crystal growth pattern changes in low molecular weight poly (ethylene oxide) ultrathin films, *Polymer* 52 (2011) 1133–1140.